Optics Communications 427 (2018) 231–237

Contents lists available at ScienceDirect

Optics Communications

journal homepage: www.elsevier.com/locate/optcom

Fourier plane imaging and illumination-direction-multiplexing using a rotating diffracting element for fourier ptychographic microscopy

Sueli Skinner-Ramos [a,b,*], Hira Farooq [a,b], Ayrton A. Bernussi [b,c], Luis Grave de Peralta [a,b]

[a] Department of Physics and Astronomy, Texas Tech University, Lubbock, TX 79409, USA
[b] Nano Tech Center, Texas Tech University, Lubbock, TX 79409, USA
[c] Department of Electrical and Computer Engineering, Texas Tech University, Lubbock, TX 79409, USA

ARTICLE INFO

Keywords:
Microscopy
Image formation theory
Illumination design
Light-emitting diodes

ABSTRACT

We demonstrate a practical method for imaging periodic structures with periods beyond the Rayleigh resolution limit of the imaging system employed. The sample was simultaneously illuminated from several directions using a combination of a source of collimated white-light, a diffracting element, and a microscope objective lens. By rotating the diffracting element, several pairs of real plane and Fourier plane images were obtained. A high-resolution image of the periodic structure was numerically reconstructed by processing the experimental images using the Fourier ptychographic algorithm. We used the Fourier plane imaging microscopy technique to approximate the initial optical disturbance in the phase-recovery algorithm.

1. Introduction

Fourier ptychographic microscopy (FPM) is a phase-recovery technique capable of producing images with a resolution better than the Rayleigh resolution limit $\lambda/(2NA_o)$, where λ is the imaging light's wavelength in vacuum, and NA_o is the numerical aperture of the microscope's objective lens [1,2]. FPM has been implemented using both planar [1,2] and hemispherical arrays of light emitting diodes (LED) [3,4], as well as liquid crystal displays [5] with visible [1–3,5] and infrared light [4,6]. FPM is based on the collection of several low-resolution images formed at the microscope's real plane (RP), where each image is obtained by illuminating the sample from a different direction. Originally, FPM was developed assuming that the incident illumination originated from a single direction at the time [1–6]. Implementing the FPM technique using LEDs proved to be very time consuming since many images had to be collected and long exposure times were required due to the low intensity of the LEDs. A natural solution to speed up the process was to illuminate the sample simultaneously from multiple directions at the same time; as such, a FPM phase-recovery algorithm capable of illumination-direction multiplexing (IDM) was previously demonstrated using planar and hemispherical LED arrays [7–9]. Fourier plane imaging microscopy (FPIM) is a technique capable of detecting the presence of periodic structures with a period beyond the Rayleigh resolution limit by using the information contained in images formed in the microscope's Fourier Plane (FP) [10,11]. In this work, we make two novel contributions to the growing body of research dedicated to the FPM technique. First, we used the light diffracted by a rotating Ronchi Ruling grating to illuminate the sample. That is, a collimated white-light beam incident on a rotating diffraction element (Ronchi Ruling grating) produced three diffraction beams incoherent with each other, which were used to illuminate the sample simultaneously from three different directions. When the diffraction element rotates, the diffracted beams also rotate describing a hollow-cone of light, which is similar to the one produced by a ring-shaped condenser. This is a useful, cost effective, and easy to implement illumination source that can provide variable illumination-direction control. Second, we used the FPIM technique to obtain detailed information contained in the collected FP images and use it to construct a better first-approximation optical disturbance for the FPM phase-recovery algorithm. Combining both innovations, we were able to obtain high-resolution images of a structure with features below the Rayleigh resolution limit. The remainder of this paper is organized as follows: In Section 2 we describe the experimental set-up used in this work. In Section 3 we present simulations obtained with a combination of the FPIM and FPM techniques. The results obtained processing the experimental images with a combination of the FPIM and FPM techniques are shown and discussed in Section 4. Finally, the conclusions of this work are presented in Section 5.

2. Experiment

Fig. 1 shows a schematic illustration of the experimental setup. We used a Nikon Elipse Ti inverted microscope mounted with a numerical aperture $NA_o = 0.15$ collection objective lens.

* Corresponding author at: Department of Physics and Astronomy, Texas Tech University, Lubbock, TX 79409, USA.
E-mail address: s.skinner-ramos@ttu.edu (S. Skinner-Ramos).

https://doi.org/10.1016/j.optcom.2018.06.051
Received 20 March 2018; Received in revised form 15 June 2018; Accepted 18 June 2018

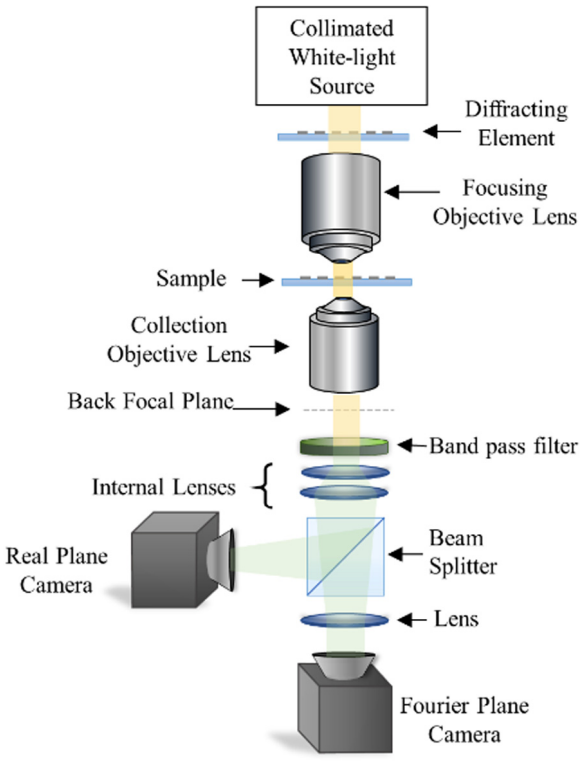

Fig. 1. Schematic illustration of the experimental setup.

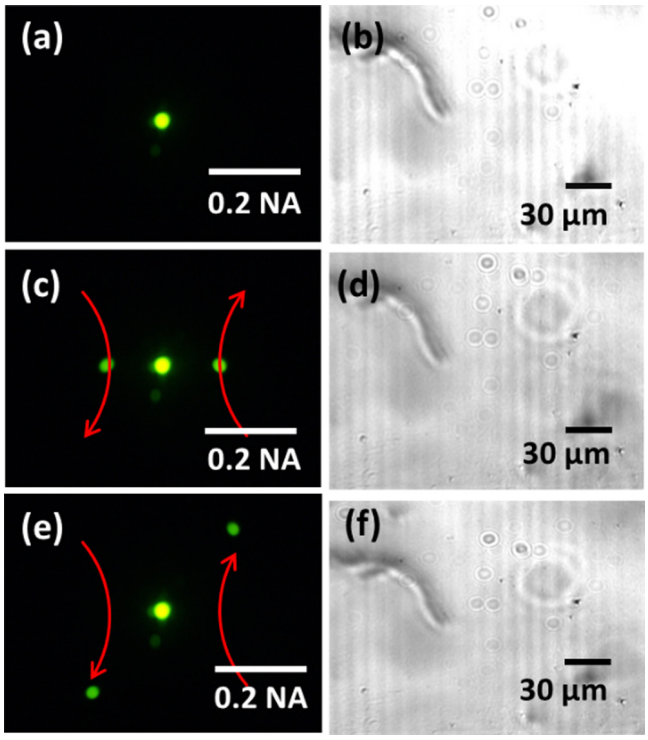

Fig. 2. (a–b, c–d, e–f) Examples of experimental pairs of (a, c, e) FP and (b, d, f) RP images obtained using (a–b) perpendicular illumination and (c–f) diffracted light by the diffracting element rotated (c–d) 0 and (e–f) 18 degrees. Superposed arrows in (c) and (e) indicate the displacement of the first-order diffraction spots.

As Fig. 1 shows, we have attached two charge-coupled device (CCD) cameras to obtain RP and FP images of the sample. The sample is illuminated by a collimated white-light source that is first directed through a diffracting element (a 100 lines/mm Ronchi Ruling grating), then focused by an objective lens with 0.3 numerical aperture. The focusing objective is placed between the diffracting element and the sample at a convenient distance to avoid projecting an image of the diffracting element onto the sample and generating a possible Moiré pattern. A band-pass spectral filter centered at $\lambda = 570$ nm wavelength with a 10 nm bandwidth was inserted after the objective lens to select a narrow frequency band of the diffracted light. Under these conditions, the resolution limit of the condenser–microscope arrangement is calculated as $\lambda/(2NA_o) = 1.9$ µm. A 600 lines/mm Ronchi Ruling grating was used as the sample to image since its period is less than the calculated Rayleigh resolution limit ($p = 1.67$ µm $< \lambda/(2NA_o)$), yet still above of the theoretical resolution limit of the condenser–microscope setup $\lambda/(NA_o + NA_c) \sim 1.43$ µm, where NA_c is the numerical aperture of the condenser. Since the sample's patterned structure was not visible, a mark was made across the patterned structure to create a large feature to help to focus the light on the sample's surface.

Nine pairs of FP-RP images were obtained by rotating the diffracting element from 0 to 180 degrees in 18-degrees angle steps and taking the corresponding images at each orientation. Fig. 2 shows representative pairs of FP-RP images obtained with the experimental setup sketched in Fig. 1. The FP-RP image pairs in Fig. 2 were obtained by taking images with perpendicular illumination (Fig. 2(a) and (b)), diffracted light by the diffracting element rotated by 0 (Fig. 2(c) and (d)), and 18 degrees (Fig. 2(e) and (f)). As expected, only the large feature at the top left of the RP images, which was introduced for focusing purposes, is visible in the experimental RP images. The sample's periodic structure with $p = 1.67$ µm is not visible because $p < \lambda/(2NA_o)$. It should be noted that the apparent large-period ($p = 10$ µm) seen in the images in Fig. 2(b), (d), and (f) is not the sample structure, rather artifacts. This is confirmed by the absence of the corresponding diffraction spots in the FP image shown in Fig. 2(a) which was produced by perpendicular illumination. Only a periodic structure with $p = 1.67$ µm was seen when we observed the sample under perpendicular illumination using a $NA_o = 1.3$ objective lens. This further confirms the inexistence in the sample of the apparent periodic structure with a period of ~10 µm. We pieced together the trajectories of the first-order diffraction spots as they moved across the FP (shown by the red arcs in Fig. 2), and from them determined that their corresponding numerical aperture was $NA_c = 0.25 > NA_o$. It should be noted that the zero-order diffraction spots corresponding to the observed first-order diffraction spots were not collected by the objective lens in this experimental arrangement because $NA_c = 0.25 > NA_o$. The zero-order diffraction spot observed in the center of the FP images shown in Fig. 2(a), (c), and (e) is produced by the light that passed without diffraction to the collection objective lens. Only the images taken with the diffracting element within ±20 degrees angle of rotation produced the first-order diffraction spots inside the numerical aperture and therefore carried information about the sample structure. The position of the diffraction spots and their trajectory in the FP during the rotation of the diffracting element can be better understood using the schematic shown in Fig. 3.

Fig. 3(a) shows a representation of the propagation of the collimated beam that is incident on the diffracting element. The three arrows shown in Fig. 3(a) exiting the diffracting element represent the trajectory of the first-tier zeroth and first-order diffraction beams. The sample is thus simultaneously illuminated from three different directions. The degree of coherence between the three diffracted beams was very low if any. This is confirmed by the observation of an image of the sample in the RP images shown in Fig. 2(d) and (f). If the degree of coherence between the beams was very high, then an image of the sample would not be seen, rather a Moiré pattern would be observed in the experimental RP images [12,13]. The lack of observation of Moiré patterns and speckles in the RP images shown in Fig. 2(d) and (f) signifies a lack of coherence between the three diffracted beams produced by the diffracting element.